**LHCb Collaboration**

LHCb 2001-009
Muon
16 June 2001
Updated version

# Muon Identification in LHCb

**Érica Polycarpo, João R. T. de Mello Neto**
LAPE - Instituto de Física - Universidade Federal do Rio de Janeiro

**Abstract**

A muon identification algorithm is presented. Both muon identification and pion misidentification are studied and the implementation of the MUID package within the SICBDST framework is described.

# 1 Introduction

The muon detector [1] is used for triggering and for muon identification. Good muon identification is very important for the reconstruction of physics channels with muons in the final state, as well as for flavour tagging of the initial b quark. For rare decays, such as $B_s \to \mu^+\mu^-$, it is fundamental to have a high muon identification efficiency while keeping the misidentification of other particles, mainly pions, as low as possible.

This work presents results obtained with a realistic muon identification algorithm for the LHCb experiment. The procedure operates on well reconstructed tracks (AXTK$QUAL=1) within the Muon System acceptance. The extrapolation point is required to be within the M2 and M3 geometrical acceptance. The tracks must also originate from the interaction region (first measured point inside VELO) and have a minimum momentum of 3 GeV/c. The minimum momentum is defined as the momentum needed to $\sim 50\%$ of the muons to arrive in M3, shown in figure 1. In the $B_s \to \mu^+\mu^-$ analysis, only tracks with momentum above 4 GeV/c are selected. In the Technical Proposal, a $p_T$ cut of 1.5 GeV/c is applied to the flavour tagging muons, leading to a minimum momentum of $\sim 4.5$ GeV/c.

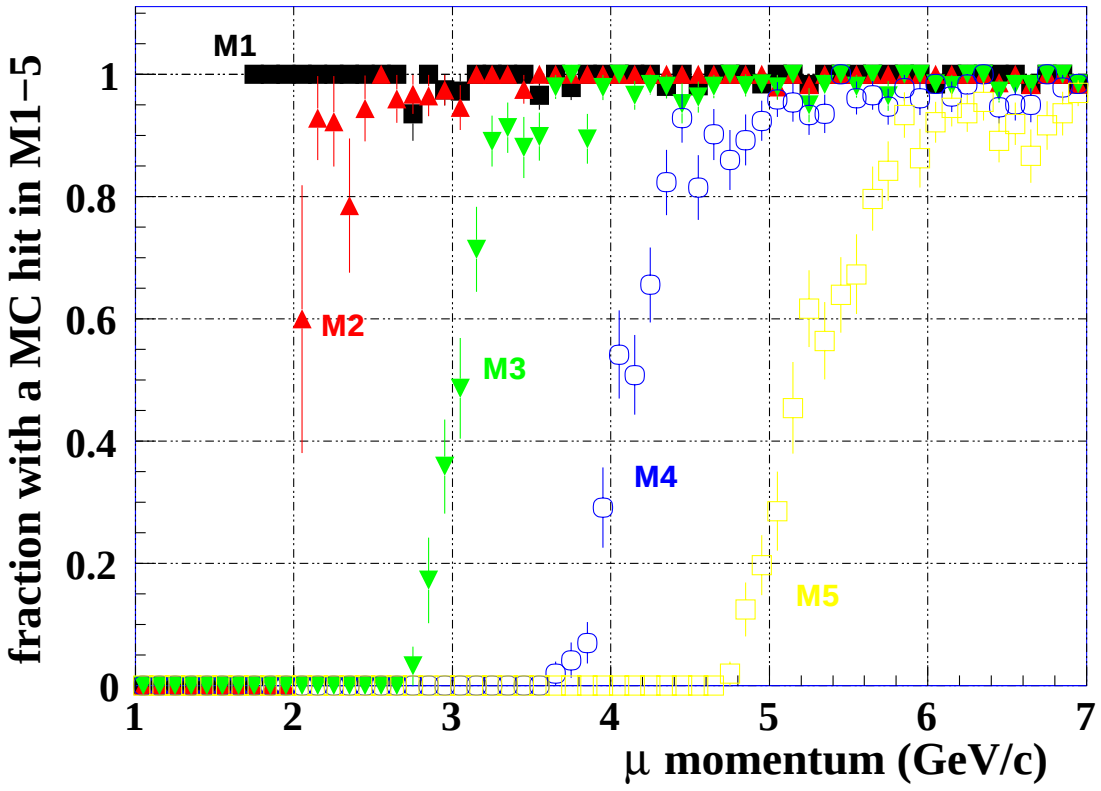


Figure 1: Fraction of muons which arrive at each of the five muon stations as function of momentum.

# 2 Data

About 4500 $b \rightarrow \mu X$ events, 120K single pions and 120K single muons were generated in LAPE (Rio de Janeiro), using SICBMC V233 and SICBDST V235 [2, 3]. The single pions and muons are generated flat in momentum $(1 \leq p \leq 150)$ GeV/c and flat in the polar angle $(0 \leq \theta \leq 250)$ mrad.

In this work, the single particle sample is used whenever the behavior of the efficiencies is given as function of the momentum of the particles. Total efficiencies or misidentification rates are given for the $b \rightarrow \mu X$ sample, which takes into account the more realistic momentum spectrum.

# 3 Algorithm

The tracks satisfying the requirements described in section 1 are linearly extrapolated from T10 to each of the muon stations. A field of interest (FOI) is defined around the extrapolation point in each station. A muon candidate is a track with a set of hits within the FOI in a minimum number of muon stations.

In order to define the FOI and the minimum number of stations required to have hits within the FOI, the muon efficiency is kept as high as possible in the entire momentum range, while the pion misidentification is kept at the level of 1-2%.

From section 3 to 5, the reference sample used to calculate the muon efficiencies is defined as muons which hit M3 (as done in reference [5, 6]) and the reference sample used to calculate the pion misidentification rate is defined as pions which hit M1. Those definitions allow the quotation of numbers which reflect the performance of the Muon System alone. In section 6, the results are given in the context of the physics analysis in LHCb.

## 3.1 Optimization of the FOI

The sample of *single muons* is used to optimize the FOI in each region of each station of the Muon System as a function of the momentum. Since the multiple scattering angle decreases with increasing momentum, hits from particles in the same muon station and region are searched for within a field of interest which decreases with increasing momentum.

To determine the FOI, the ratios

$$\frac{|\Delta x|_{MC}}{xpad} = \frac{x_{MCpad} - x_{extrapolation}}{xpad} \text{ and } \frac{|\Delta y|_{MC}}{ypad} = \frac{y_{MCpad} - y_{extrapolation}}{ypad}$$

are studied as a function of momentum, in each region of each station. In the expression above $xpad$ is the $x$ dimension of the pad and $x_{MCpad}$ is the $x$ position of the pad which is actually hit by the particle which produces the track (the same for the $y$ coordinate). The distance $|\Delta x|_{MC}$ takes into account multiple scattering and pad granularity. In figure 2 the scatter plots

$$\frac{|\Delta x|_{MC}}{xpad} \times p \quad \text{and} \quad \frac{|\Delta y|_{MC}}{ypad} \times p$$

are shown for region 3 of station 3, together with the corresponding profile histograms. For each momentum bin, the $RMS$ and the mean value of the ratios are recorded. Then the function

$$\frac{\Delta x^{n}_{foi}}{xpad}(p) = a_0 + a_1 p + a_2 \exp(a_2 p)$$

is fitted to the points given by

$$(mean + \ n \ \times RMS)$$

in each momentum bin, with $n = 2, 3$ or 4. The fitted curves $\frac{\Delta x^n_{foi}}{xpad}(p)$ for $n = 2$ to $4$ are also shown in figure 2. For a particle with momentum $p$, hits are sought with ratios $\frac{|\Delta x|}{xpad}$ and $\frac{|\Delta y|}{ypad}$ smaller than the values of $\frac{\Delta x^n_{foi}}{xpad}(p)$ and $\frac{\Delta y^n_{foi}}{ypad}(p)$. Therefore, in each muon station, the value of $\frac{\Delta x^n_{foi}}{xpad}(p)$ and $\frac{\Delta y^n_{foi}}{ypad}(p)$ will depend on the momentum of the particle and on the Muon System region it traverses.

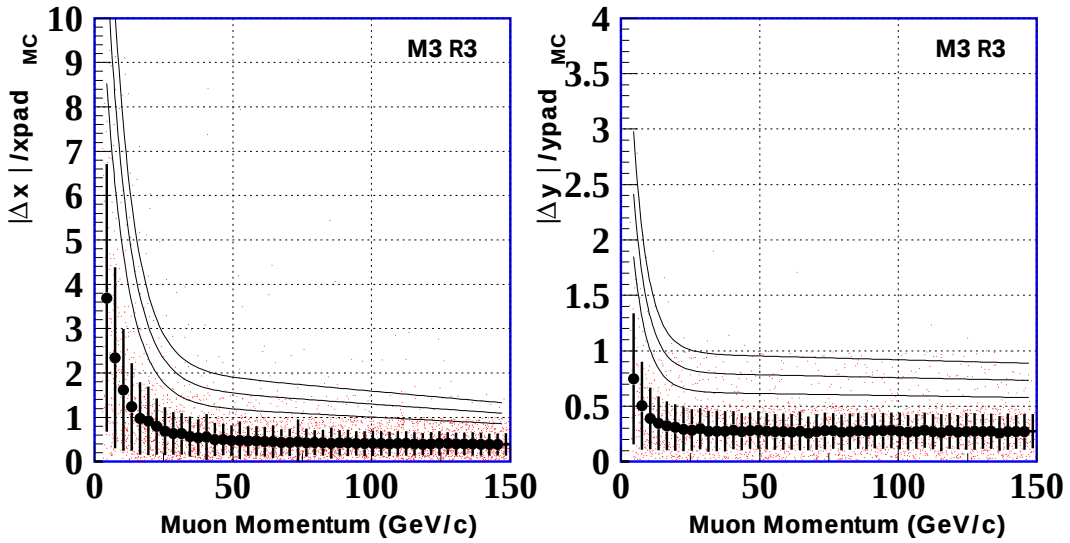


Figure 2: Scatter plots of the ratios $|\Delta x|_{MC}/xpad$ and $|\Delta y|_{MC}/ypad$ as a function of momentum in region 3 of station M3. The profile histogram is superimposed. The solid lines are the results of the fits $\frac{\Delta x^n_{foi}}{xpad}(p)$, for $n = 2$ to $4$, with n=2 for the curve closest to the profile histogram.

The plot in figure 3 shows the fraction of muons with at least one hit within the FOI in M2 *and* M3. The relative difference between the muon fractions when using 3 or 4 $RMS$ FOI is below 2% in the whole momentum spectrum, while the difference between 2 and 4 $RMS$ is $\sim$ 11% in the lowest momentum bin. The total pion misidentification in the $b \rightarrow \mu X$ sample (concentrated in the low momentum range) is kept below the 2% level in all the three options. By requiring a hit in M2 *and* M3 within a 3 $RMS$ FOI around the extrapolation point, the muon efficiency can be kept above the 95% level. Hence, the 3 $RMS$ FOI is the one chosen as the standard FOI in this muon identification procedure. The reduction of the pion misidentification can be achieved in additional steps, that can be more easily tuned by the users of the muon identification procedure.

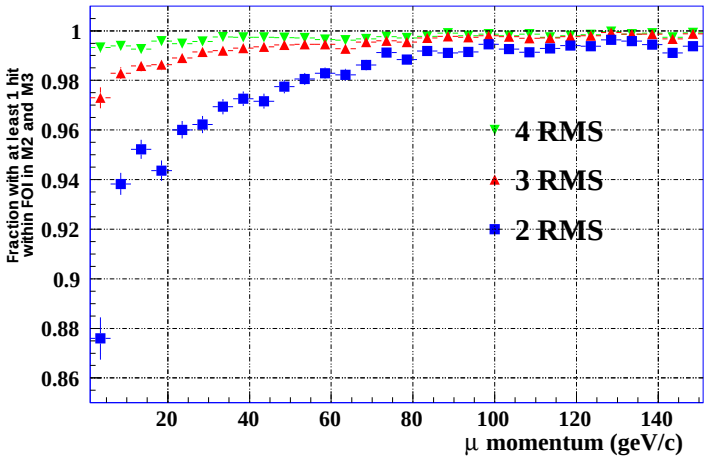


Figure 3: Fraction of muons with at least one hit within the FOI in M2 and M3 as function of their momenta. Note that the $y$ scale starts at 85%.

To further improve the robustness of the algorithm, the requirement on the number of stations fired within the FOI is studied. Figure 4 shows the efficiency for muons of the single sample when requiring

1. 2 stations : $M2 + M3$;
2. 3 stations : $M2 + M3 + (M4$ or M5);
3. 4 stations : $M2 + M3 + M4 + M5$;

fired within a 3 $RMS\,FOI$ around the track extrapolation. The second plot shows only the low momentum part of the total spectrum given in the first graphic. Above 6 GeV/c, the requirements of 2 and 3 stations are compatible for muons, while requiring 4 stations becomes compatible with them only above 40 GeV[1].

Hence, it is natural to define as final requirement the momentum dependent criteria :

| | | |
|---|---|---|
| $M2 + M3$ | for | $p <$6 GeV/c; |
| $M2 + M3 + (M4$ or M5) | for | 6 GeV/c $< p <$ 40 GeV/c; |
| $M2 + M3 + M4 + M5$ | for | $p >$ 40 GeV/c; |

The relevant efficiencies obtained in the $b \rightarrow \mu X$ sample are given in table 3.1 together with the efficiencies expected for a minimum hardware efficiency per station equal to 99%, which is required for triggering. The total muon efficiency drops by only 1% from requirement 1 to 4. Since requirement 4 keeps the procedure more robust against random combinations of background hits[2] [4] it is the one used to define a muon candidate.

[1] See Addendum.

[2] Hits added by the Muon Background package.

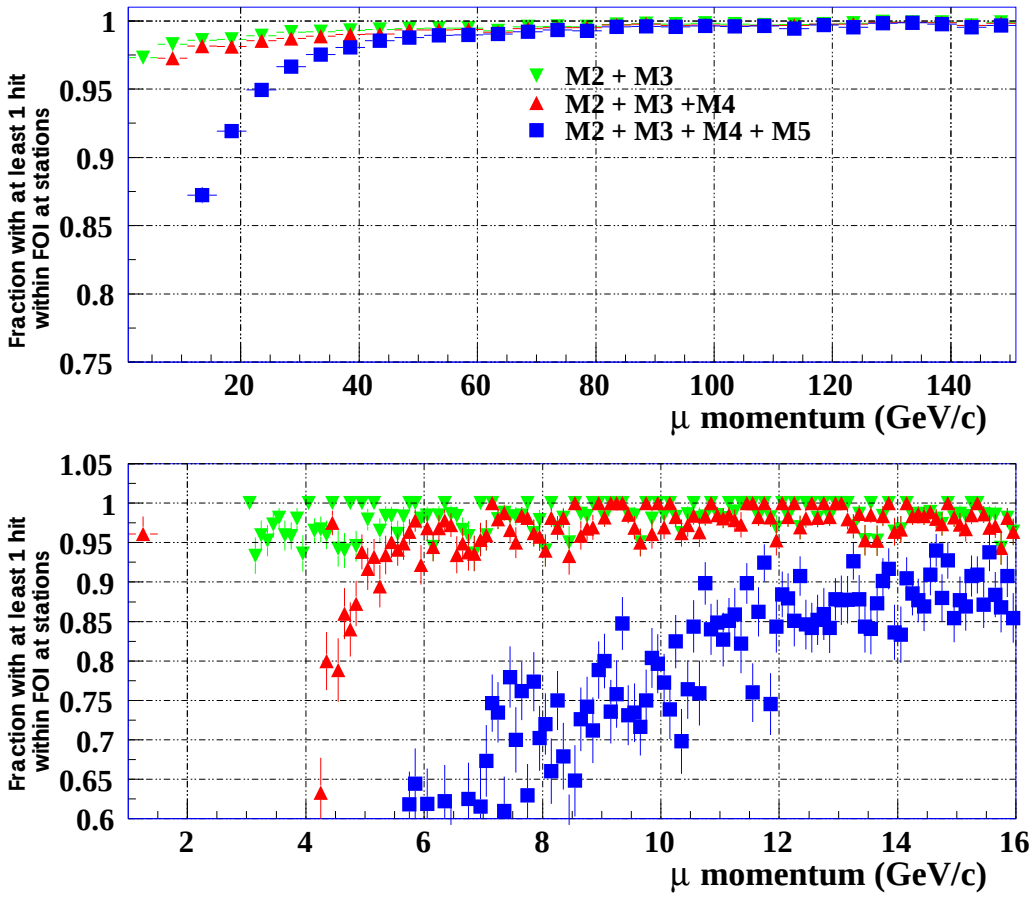


Figure 4: Fraction of muons with hits within the 3 RMS FOI in three different combinations of stations. The bottom plot is a *zoom* of the low momentum part of the spectrum in the top plot.

| Particle | Requirement 1 | Requirement 2 | Requirement 3 | Final Requirement |
|---|---|---|---|---|
| Muon | 97.0± 0.5 % | 91.0± 0.8 % | 74.8 ± 1.2 % | **96.0± 0.5 %** |
| Pion | 0.70± 0.04% | 0.45± 0.03 % | 0.19 ± 0.02% | **0.62 ± .03%** |
| Chamber efficiency | $>$ 98 % | $>$ 98 % | $>$ 96 % | 96-98 % |

Table 1: Relevant efficiencies in the $b \rightarrow \mu X$ sample. The third row is given by the logic combination of the chamber efficiencies of the stations used in the different requirements.

# 4 Composition of the misidentified pion sample

After the momentum dependent requirement described in the previous section, the muon efficiency is $96.0 \pm 0.5$ % and the pion misidentification is $0.62 \pm 0.03$ %. Only 8% of these remaining pions were misidentified due to background hits found within the FOI in at least one of the muon stations and 84% of them are misidentified due to muon hits in all required stations. From those, 30% are muons produced in the direct decay in flight of the pions which are being extrapolated to the Muon System. The decay occurs between M1 and M2 (recall that we require the pion to reach M1). The other 70% are mainly muons produced in the decay of other pions and kaons that happen to be in the same direction of the pion analyzed. There is also a contribution from muons produced in the decay of D and B mesons close to the interaction point ($\sim$ 20% of those 70%). Figure 5 shows the $xz$ position where the muons which fire the pad closest to the pion extrapolation point in M2 are produced. The dots show muons produced in the decay of particles in the same direction as the pion and two muons produced in the decay of hadrons from the calorimeter cascade (punch-through).

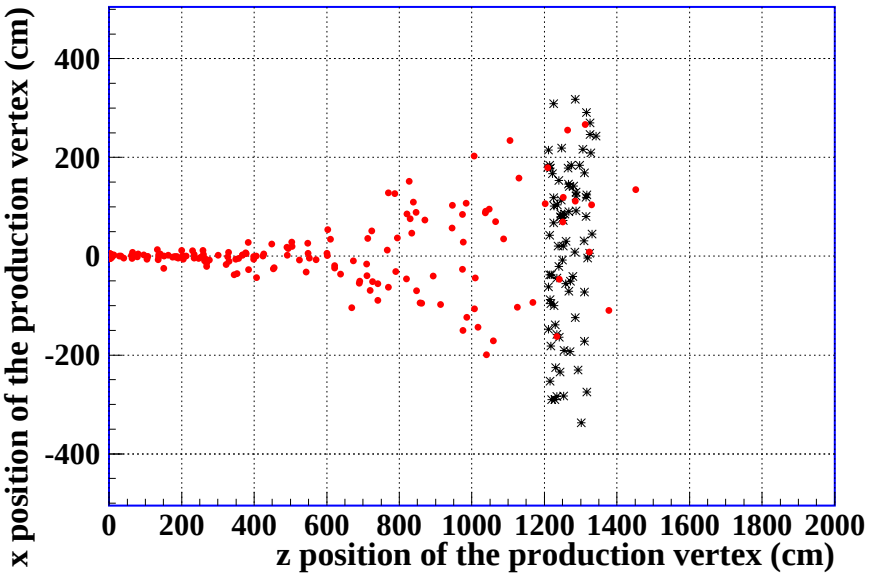


Figure 5: Position of the production vertex of the muons which fire the pad closest to the extrapolation point of the pions seen as muon candidates. The asterisks show muons produced in the decay in flight of the pion, the dots are the other contributions.

The other 8 % of the pions are misidentified basically due to random combinations of punch-through hits and *ghost* hits. The *ghost* hits are an artifact of the Muon System digitization, which combines strips in the $x$ and $y$ directions to find the fired $pads$.

Figure 6 shows how the use of FOI reduces the punch-through in the muon stations. Table 4 summarizes the composition of misidentified pion sample.

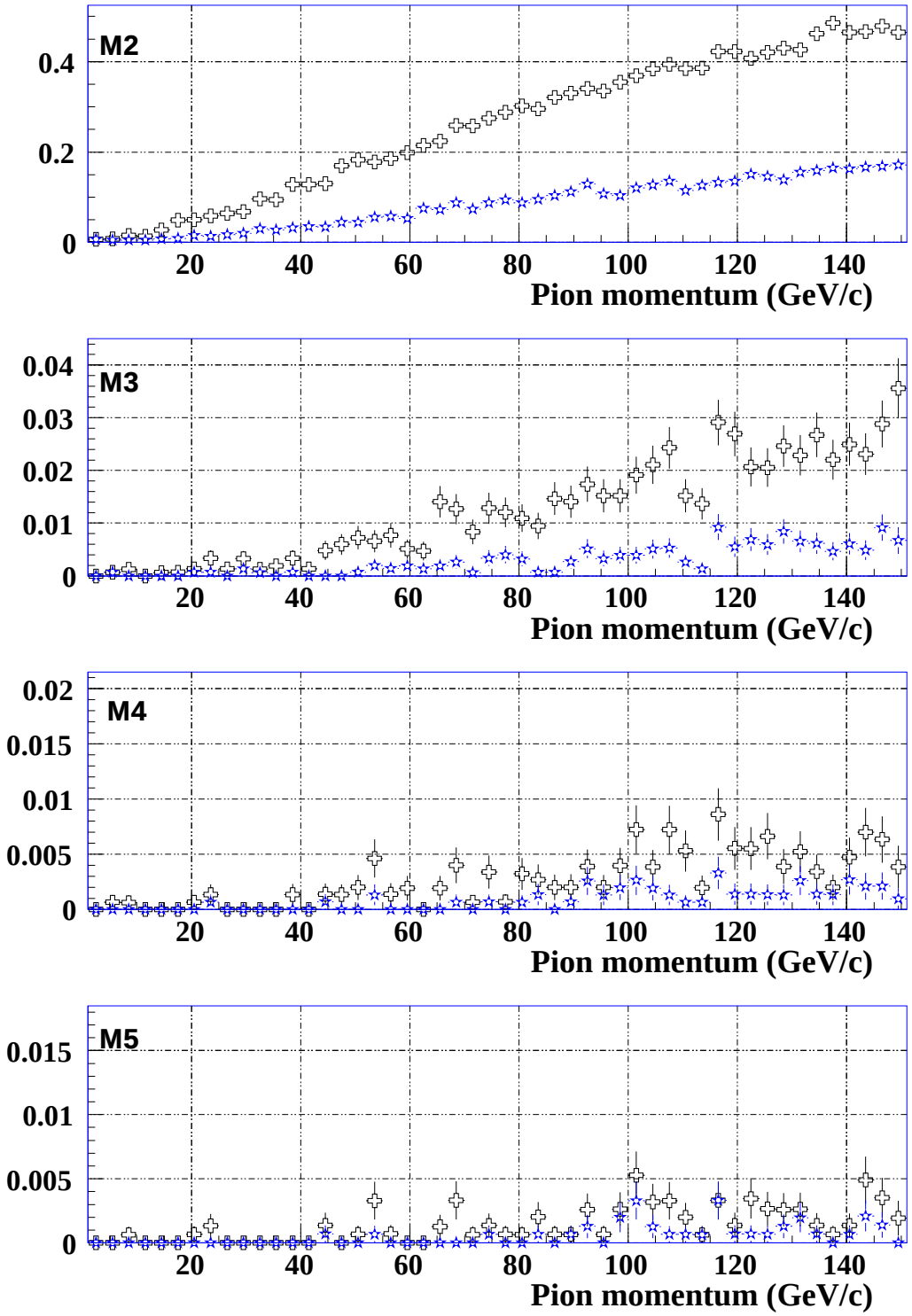


Figure 6: Punch-through in the muon stations after the calorimeter, as function of the momentum of the pions. The crosses give the probability to find a hit in the station when a pion is sent through the detector and the stars give the probability to find a hit within the FOI.

| Source of pion misidentification | fraction |
|---|---|
| muons | 84 % |
| from pion decays in flight | 30 % |
| from hadron decays in the same direction of the pion | 70 % |
| random combination of hits | 16 % |
| with at least 1 background hit in any of the stations | 50 % |
| with at least 1 punch-through or ghost hit | 50 % |

Table 2: Contribution of the different sources of pion misidentification to the total fraction of pions misidentified.

# 5 Discriminating variables

In order to assign a confidence level to the muon candidates that can help in the further reduction of the pion misidentification several variables were studied. From those, only the ones with some discriminating power are presented here:

- $\Delta S_x$ : difference between the slopes $S_x$ given by the tracker system at T10 and the one calculated with the pads closest to the extrapolation point in M2 and M3 [5].

- $< \frac{\Delta x}{xpad} >= \frac{1}{N} | \sum_{i=1}^{N} \frac{\Delta x_i}{xpad} |$ : ratio between the signed distance from the closest pad to the extrapolation point in the bending direction, averaged over the stations with hits within the FOI.

Figure 7 shows the $\Delta S_x$ distribution for muons and pions in the $b \rightarrow \mu X$ sample. Each style represents one region of the system. Since the pad sizes increase from the inner region to the outer region, the average difference in the slopes increases accordingly in the muon sample. For pions this behavior is much less evident, due to the random combination of hits from different sources. The plots in figure 8 give the muon efficiency and the pion misidentification as a function of the cut in $\Delta S_x$ smaller than the value in the horizontal axis. In the bottom plot, the confidence level based on $\Delta S_x$ is used instead of the value of the variable itself. A cut that gives 90% muon efficiency results in a total pion misidentification of $\sim 0.45$%.

Figure 9 shows the distribution of $< \frac{\Delta x}{xpad} >$. This variable is built in order to reduce the contamination from decays, which would have larger values due to distances from the extrapolation to the hits with the same sign in all stations. Figure 10 shows the discriminating power of both the $\Delta S_x$ and the $< \frac{\Delta x}{xpad} >$ variables. The pion misidentification is plotted against the muon efficiency for different cuts in the variables. One can notice that, if purity is more important than efficiency, the cut in $< \frac{\Delta x}{xpad} >$ is more adequate than the cut in $\Delta S_x$. Using both cuts together, keeping the total final muon efficiency at 90 %, the relative reduction in the pion misidentification is of 5 %, as compared to the cut in $\Delta S_x$ only.

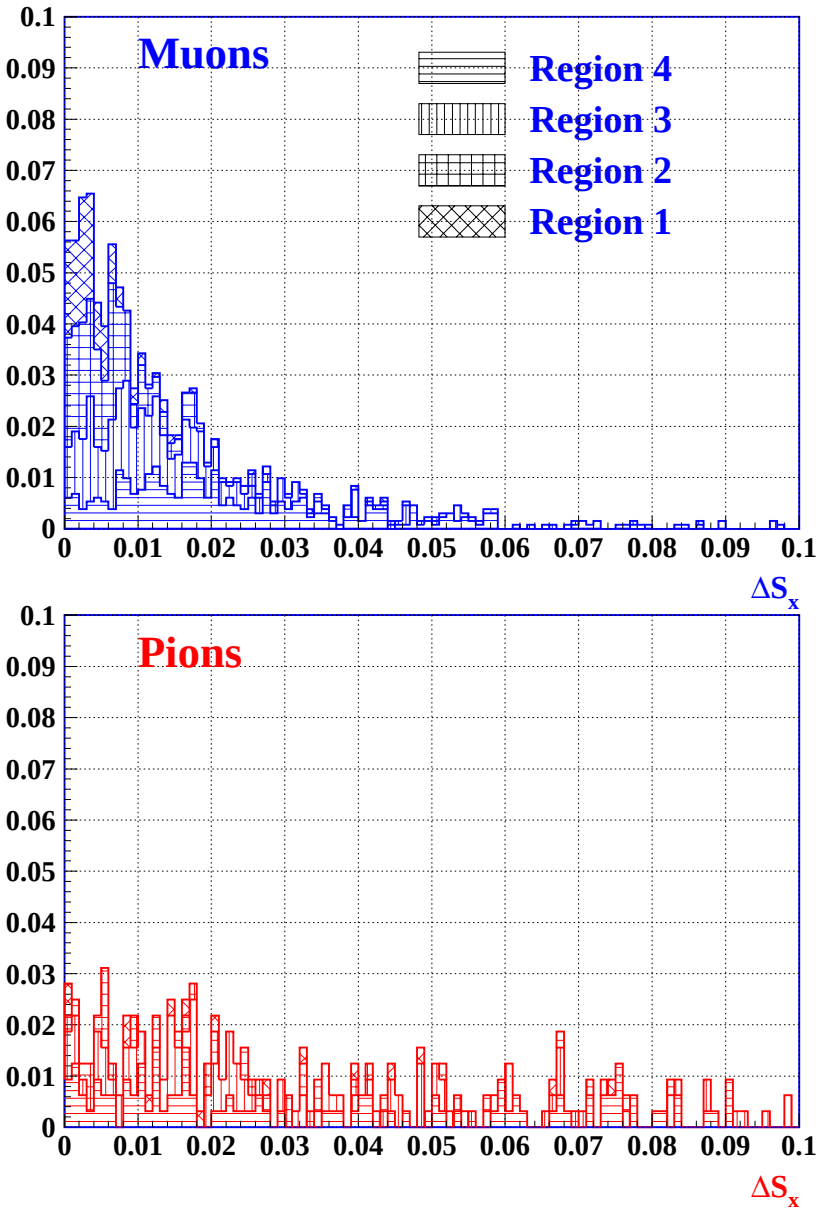


Figure 7: Difference between the $x-z$ slopes of the tracks in T10 and calculated with hits found within the FOI in M2 and M3. The contributions from the different regions are added and not superimposed. In the top plot, the tracks in region 1 are shown in the upper most distribution.

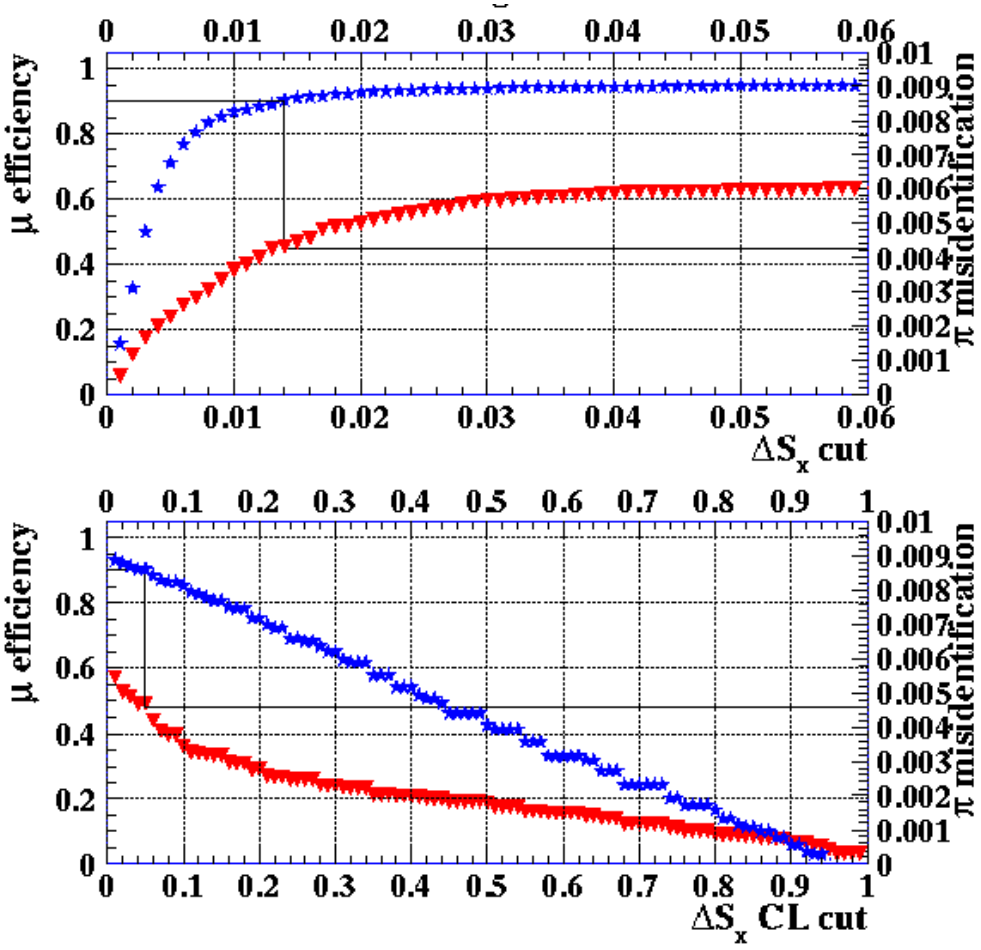


Figure 8: The top plot shows the muon efficiency (stars in the left axis) and the pion misidentification (triangles in the right axis) after a cut in the value of $\Delta S_x$ smaller than the value in the horizontal axis. The bottom plot shows the same information in the vertical axis for a cut in the confidence level based on $\Delta S_x$.

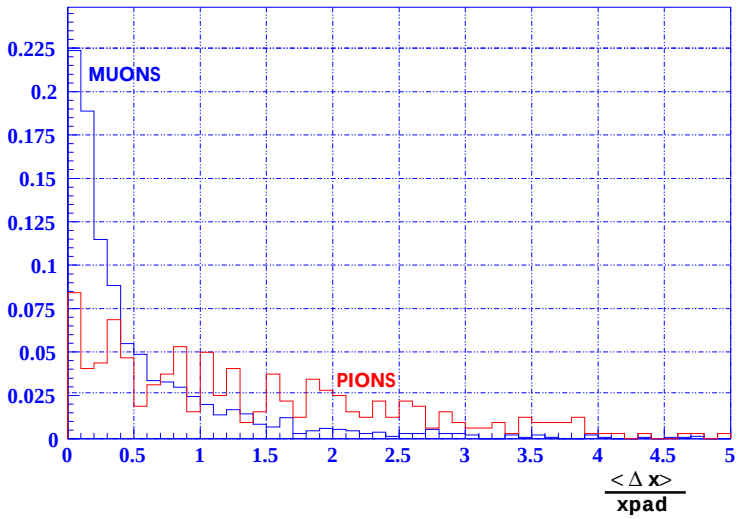


Figure 9: Ratio of the distance between the extrapolation point and the closest pad to the pad size in the $x$ direction, averaged over the stations which have the closest pad within the FOI.

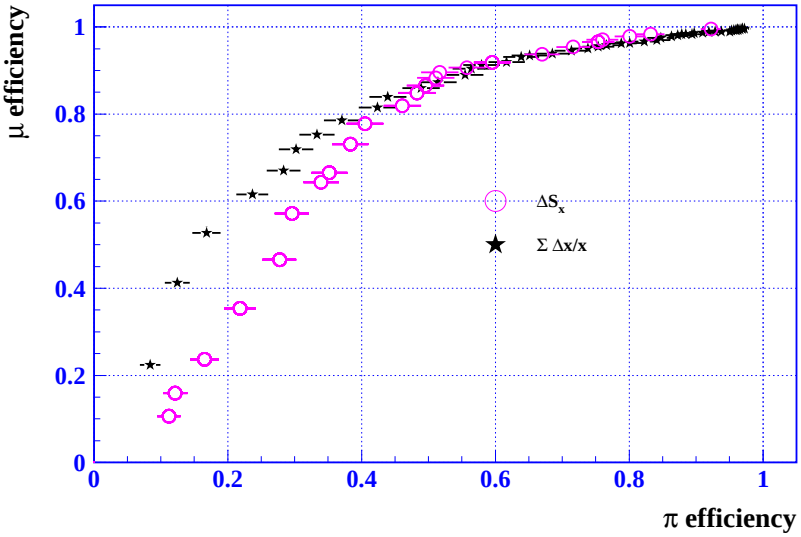


Figure 10: Muon efficiency plotted versus the pion efficiency for increasing cuts on $\Delta S_x$ and $< \frac{\Delta x}{xpad} >$.

# 6 Performance of the Muon ID procedure for Physics Analysis

For physics studies, the relevant efficiencies are those calculated with particles satisfying the requirements in sec. 1 only, without verifying if the particle reaches the Muon System. In this case, the final muon efficiency is reduced due to particles lost between the interaction point (IP) and M3. The pion misidentification is increased, due to decays in flight between the IP and M1. The dependence of these quantities on the particle momentum is shown in fig. 11. The total efficiency in the $b \to \mu X$ sample is $94.0 \pm 0.6$ % for muons and $1.49 \pm 0.5$ % for pions. The pion contamination comes in 90 % of the cases from candidates with muon hits in all stations. About 70 % of those candidates are muons coming from the decay in flight of the pion which is being extrapolated to the Muon System, while the other 30 % come from muons which happen to be in the same direction of the pion. In fact, the muon candidate is a true muon in the Muon System, but matching a pion track in the LHCb Tracker. Once again the contribution from background hits to the pion contamination is low, of the order of 5 %. The remaining 5 % of the pions are seen as muon candidates due to combination of punch-through hits and *ghost* hits. Table 6 shows a summary of the different contributions. The average number of pions reconstructed per event in the $b \to \mu X$ sample is $\sim 80$ and the average number of pions which satisfy the requirements used to define the reference sample is $\sim 14$. Note that the right plot of figure 11 does not include all effects, since one particle is generated per event. Hence, the contribution from particles in the same direction of the pions is not included as well as the background hits. Those effects are more important for the pions, since the muons have mainly as closest hits the ones produced due to their passage through the chambers.

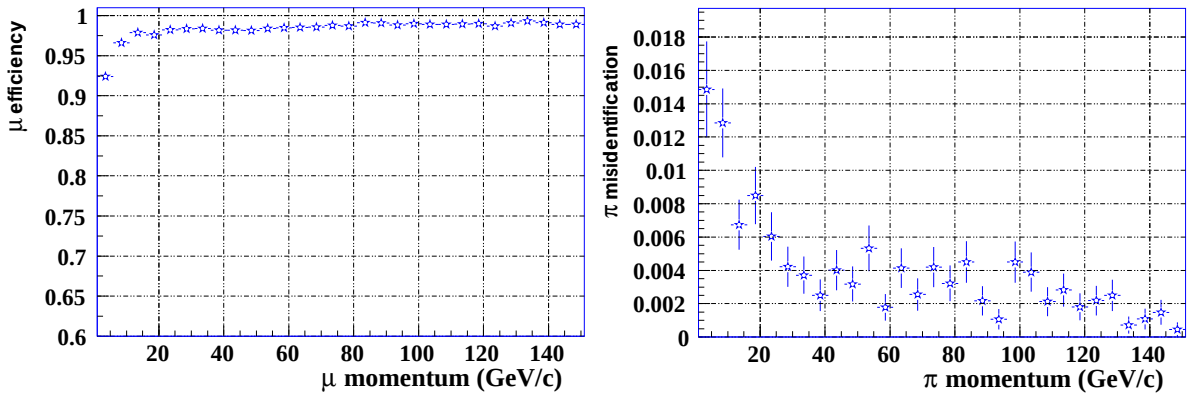


Figure 11: Muon efficiency (left) and pion misidentification (right) as function of the momentum, for particles coming from the interaction point.

| Source of pion misidentification | fraction |
|---|---|
| muons | 90 % |
| from pion decays in flight | 70 % |
| from hadron decays in the same direction of the pion | 30 % |
| random combination of hits | 10 % |
| with at least 1 background hit in any of the stations | 50 % |
| with at least 1 punch-through or ghost hit | 50 % |

Table 3: Contribution of the different sources of pion misidentification to the total fraction of pions misidentified.

A cut on $\Delta S_x$ that keeps the muon efficiency at 90% reduces the pion contamination to 1.1%.

In order to further reduce the pion contamination, we investigated a multivariate approach including information from the hadronic calorimeter and the RICH [7]. From HCAL we get the energy deposited in a nine cell cluster around the track (see figure 12). From the RICH we use the probabilities for the muon and the pion hypothesis as given in the bank RIFS (see figure 13). A three layer neural network based on JETNET[8] was set up with the following inputs for each muon candidate:

- particle momentum;
- ratio of HCAL energy to momentum of the track;
- RICH probability for muon hypothesis;
- RICH probability for pion hypothesis;
- $\Delta S_x$;
- $< \frac{\Delta x}{xpad} >$;

The output of the neural network is shown in the top plot of figure 14. One can see that there is a good separation between pions and muons. The efficiency as a function of the cut of the confidence level as given by the neural network is shown in the second and third plot for muons and pions respectively. Keeping the muon efficiency at 90% the pion contamination is reduced to 0.6%. This represents a relative gain of 45% compared to the cut on $\Delta S_x$ only.

Although this is a promising result, the multivariate approach is preliminary and is not included in the released code.

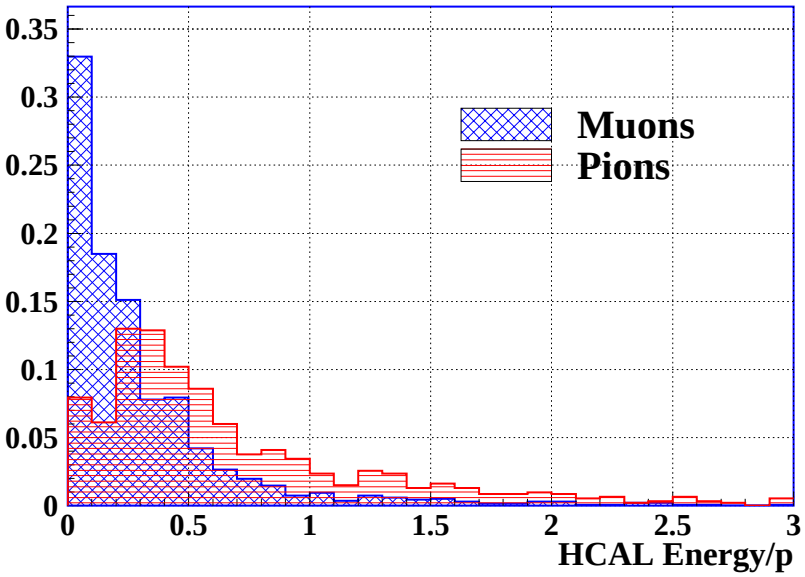


Figure 12: Ratio of the energy deposited in a nine cell cluster around the track in the hadronic calorimeter to the track momentum.

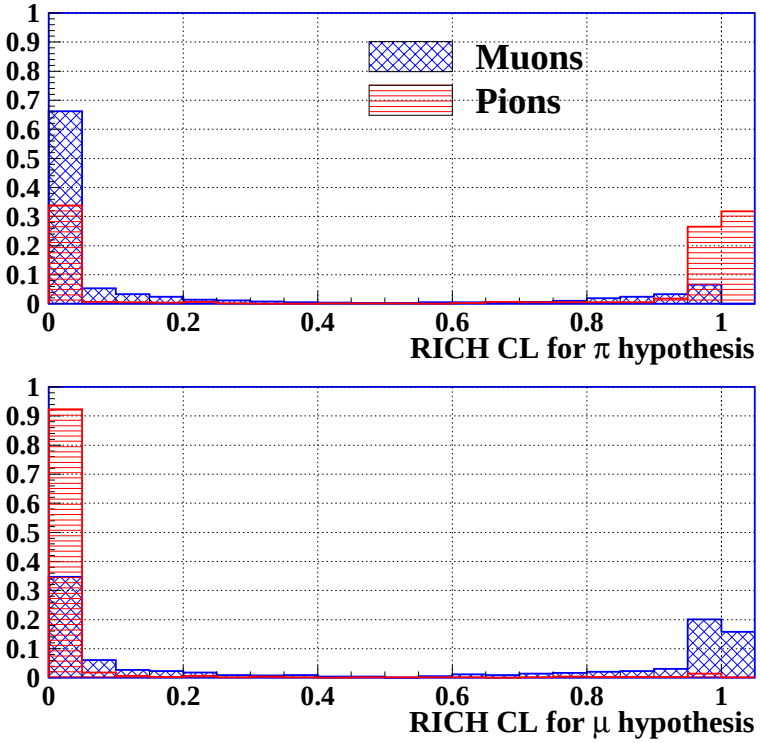


Figure 13: Distributions of the RICH probabilities for the pion hypothesis (top) and muon hypothesis (bottom). The distributions are all normalized to a total number of events equal to one. The probabilities are taken from the RIFS bank.

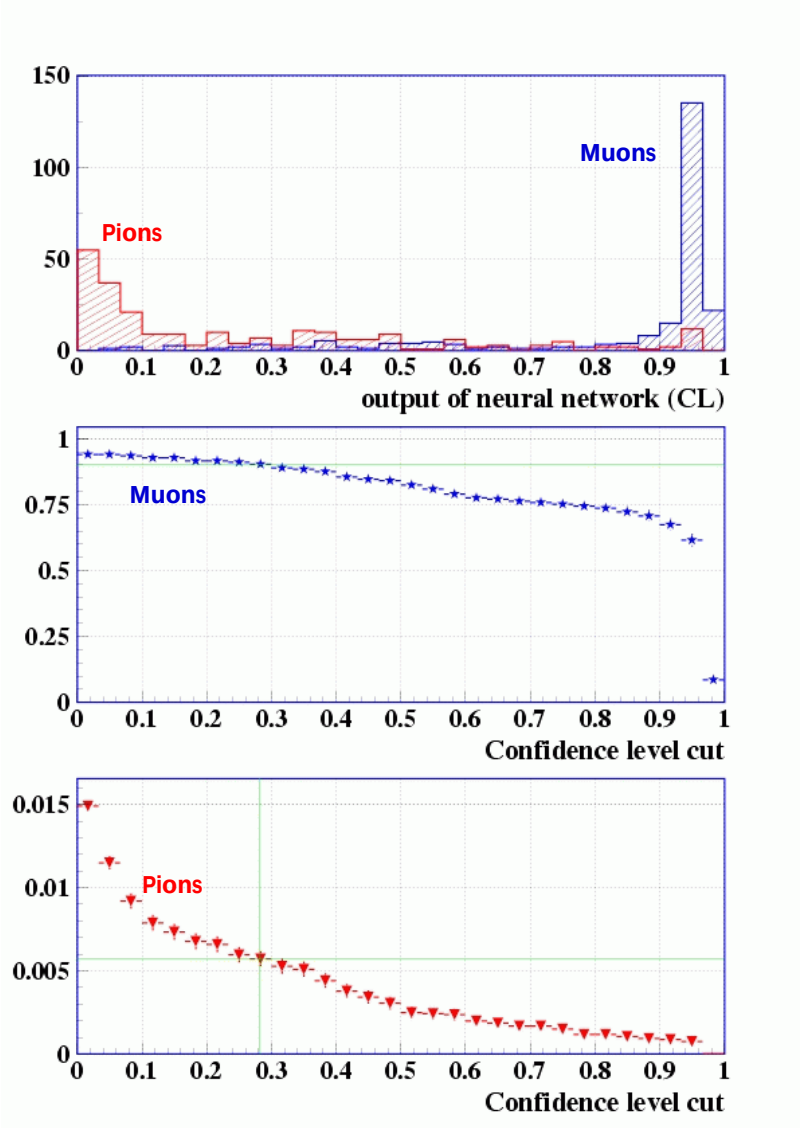


Figure 14: Output of the neural network for muons and pions (top). The muon efficiency after a cut on the neural network output larger than the value in the horizontal axis is shown in the middle plot, while the efficiency for pions is shown in the bottom plot. Note that the efficiency of the cut is multiplied by the efficiency of the muon candidate requirement.

# 7 MUID code

This algorithm has been implemented as a SICBDST package inside $recmuon/v3$. A bank called MUID is filled for each muon candidate track and has a reference to the corresponding AXTK object. The description of the bank is found below.

```
OBJECT
#
NAME:       MUID   !  Bank of Muon Candidates (accord-
ing to muon ID algorithm)
FANOUT:     MURE
AUTHOR:     E. Polycarpo, J. de Mello
VERSION:    0
PARTITIONS: 1      !
NOBJECTS:   500    !  initial number of objects
PARAMETERS: 18     !  number of parameters per object with-
out ID and refs
#
# ( Type may be F - float, I - integer, B - bit pattern, H - Hol-
lerith )
# Name Type   Min   Max  Accuracy
#
P     F   -5000.  5000.    0.01  ! muon candidate momentum
DSX   F       0.   500.   0.001  ! difference in the xz slopes
PDSX  F      -2.     2.   0.001  ! muon candidate probability
                                 ! (CL based on DSX)
DXX   F       0.   500.   0.001  ! ratio dx/padsize aver-
aged over stations
                                 ! with hits within FOI
PDXX  F      -2.     2.   0.001  ! muon candidate probability
                                 ! (CL based on DXX)
NHT1  I       0.   500.     1.0  ! number of hits in station 1 (in-
side FOI)
NHT2  I       0.   500.     1.0  ! number of hits in station 2 (in-
side FOI)
NHT3  I       0.   500.     1.0  ! number of hits in station 3 (in-
side FOI)
NHT4  I       0.   500.     1.0  ! number of hits in station 4 (in-
side FOI)
NHT5  I       0.   500.     1.0  ! number of hits in station 5 (in-
side FOI)
EHC1  F   -5000.  5000.    0.01  ! HCAL energy around the track (1 cell)
EHC9  F   -5000.  5000.    0.01  ! HCAL energy around the track (9 cells)
PREL  F       0.     1.   0.001  ! RICH RIFS prob (electron)
PRMU  F       0.     1.   0.001  ! RICH RIFS prob (muon)
PRPI  F       0.     1.   0.001  ! RICH RIFS prob (pion)
PRKA  F       0.     1.   0.001  ! RICH RIFS prob (kaon)
PRPR  F       0.     1.   0.001  ! RICH RIFS prob (proton)
MCID  I       0.   200.     1.0  ! Monte Carlo ID
#
REFERENCE:    1
```

```
AXTK
#
END OBJECT
```

# 8 Conclusions and Prospects

We presented an algorithm which is efficient for muons. The pion contamination is kept at the percent level and the major contribution to it comes from true muons crossing the Muon System, matching the pion track. The code was implemented in SICBDST and can be used in the physics analysis.

The study will be repeated with more statistics in the $b \rightarrow \mu X$ sample and possible improvements will be investigated. The performance will be analyzed with different levels of background hits and different logical layouts. We will also proceed with the multivariate approaches, like neural networks and Bayesian methods.

# 9 Addendum

After this note was written, it was noticed a mistake in plot 4. The correct plot is shown in figure 15. The efficiency for the requirement of four stations fired within the FOI is compatible with the requirement of three stations for momenta above 10 GeV/c, instead of 40 GeV/c. The results shown in this note were obtained using the 40 GeV/c threshold, even though the default threshold in the muon identification algorithm has been set to 10 GeV/c. The results with the correct threshold are similar to the ones shown here, because the contribution from particles with momentum above 10 GeV/c is small.

# 10 Acknowledgments

We would like to thank I. Korolko, T. Nakada, G. Wilkinson and the Muon group, in particular to G. Corti, K. Harrison, B. Schmidt, A. Tsaregorodtsev, P. Colrain and the other LAPE colleagues, for many useful discussions. Thanks to G. Martelotti for pointing out to us a mistake in plot 4. This work was partially supported by European Community (contract CI1*-CT94-0118), CNPq, CAPES, FAPERJ and Fundação José Bonifácio (UFRJ).

# References

[1] *LHCb Technical Proposal*, S. Amato *et al.*, CERN LHCC 98–4, February,1998.

[2] *SICb user guide*, A. Tsaregorodtsev, http://lhcb-comp.web.cern.ch/lhcb-comp/SICB/html/sicbug.html

[3] CERN Program Library Long Writeup W5013 (1993).

[4] *Muon System parameterized background - algorithm and implementation*, A. Tsaregorodtsev, LHCb 2000-11 MUON, May, 2000.

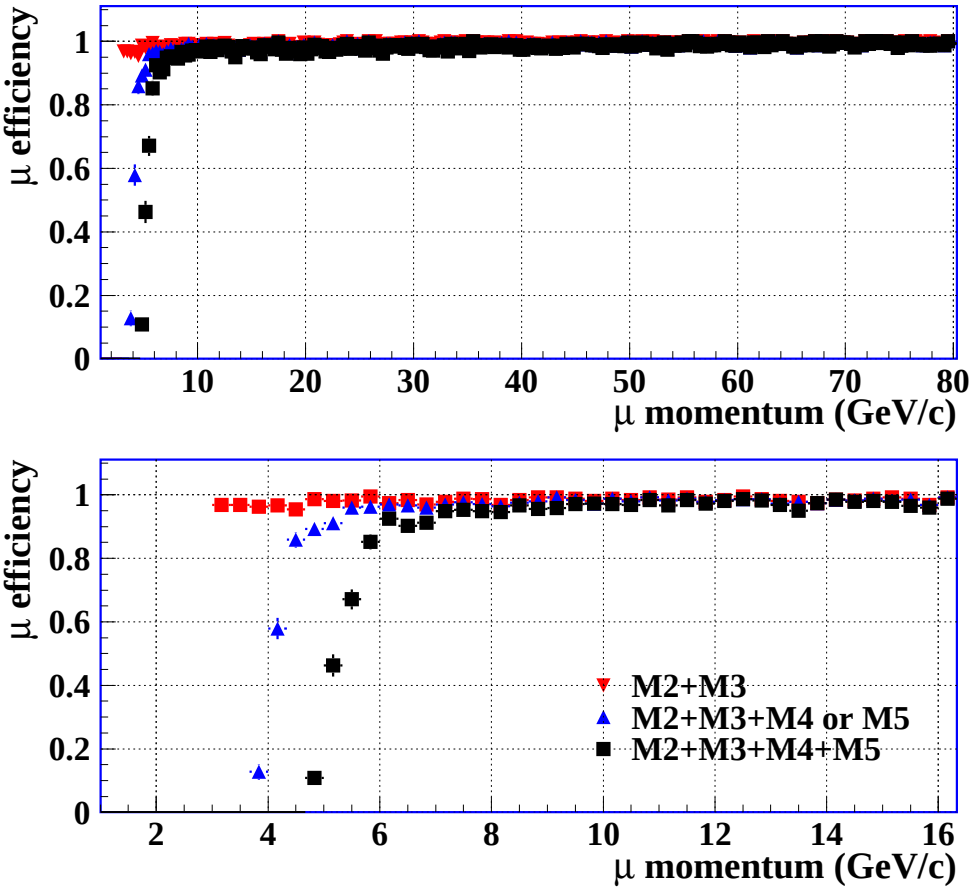


Figure 15: Fraction of muons with hits within the 3 RMS FOI in three different combinations of stations. The bottom plot is a *zoom* of the low momentum part of the spectrum in the top plot.


[5] *Optimization of muon system layout*, P. Colrain and B. Schmidt, LHCb 2000-016 MUON, January, 2001.

[6] *Montecarlo samples and efficiency definitions for the muon system optimization*, LHCb 2001-007 MUON, G. Martellotti, S. Martinez, R. Santacesaria.

[7] *Multivariate Methods for Muon ID in LHCb*, with Flavia Landim and Ana Carolina de A. Jesus, in preparation.

[8] *JETNET 3.0 - A Versatile Artificial Neural Network Package*, C. Peterson, T. Rgnvaldsson, L. Lönnblad, CERN-TH 7135/94, (1994).